



Contents lists available at ScienceDirect

Journal of the Mechanics and Physics of Solids

journal homepage: www.elsevier.com/locate/jmps

Effective toughness of heterogeneous media

M.Z. Hossain^a, C.-J. Hsueh^a, B. Bourdin^b, K. Bhattacharya^{a,*}^a Division of Engineering and Applied Science, California Institute of Technology, Pasadena, CA 91125, USA^b Department of Mathematics, Center for Computation & Technology, Louisiana State University, Baton Rouge, LA 70803, USA

ARTICLE INFO

Article history:

Received 24 December 2013

Received in revised form

15 May 2014

Accepted 11 June 2014

Available online 20 June 2014

Keywords:

Effective toughness

Brittle fracture

Heterogeneous media

Toughness asymmetry

Computational fracture mechanics

ABSTRACT

We propose a versatile approach to computing the effective toughness of heterogeneous media. This approach focusses on the material property independent of the details of the boundary condition. The key idea is what we call a surfing boundary condition, where a steadily propagating crack opening displacement is applied as a boundary condition to a large domain while the crack set is allowed to evolve as it chooses. The approach is verified and used to study examples in brittle fracture. We demonstrate that effective toughness is different from effective or weighted surface area of the crack set. Furthermore, we demonstrate that elastic heterogeneity can have a profound effect on fracture toughness: it can be a significant toughening mechanism and it can lead to toughness asymmetry wherein the toughness depends not only on the direction but also on the sense of propagation. The role of length-scale is also discussed.

© 2014 Elsevier Ltd. All rights reserved.

1. Introduction

Fracture mechanics, starting with the work of Griffith (1921), is a grand success of the past century with the development of a profound theory that can describe crack propagation in complex macroscopic situations. However, this theory requires an empirical parameter – the fracture toughness. How this parameter arises, or how it changes, or even what it means in the microstructural hierarchy of materials remains incompletely understood.

Over the last few decades a number of composite structures have been developed, especially in the context of ceramics, where microstructural features have been exploited to enhance the toughness. Consequently, there is an extensive literature on the fracture toughness of composite materials, e.g. (Bower and Ortiz, 1991; Cox and Yang, 2006; Evans and Faber, 1981; Faber and Evans, 1983, 1983; Gao and Rice, 1989; Hutchinson and Suo, 1992; Suresh, 1985). These composites also motivated systematic mathematical formulation of the change in stress intensity with perturbations in the crack front and modulus (Gao, 1991; Rice, 1985). However, this work is generally limited to particular microstructures of relevance to composites.

The relation between random microstructures and observable features including morphology of crack surfaces and rate dependence has received much attention with the discovery of some universal scaling laws (Bonamy et al., 2006, 2008; Bouchaud, 1997; Ponsion and Bonamy, 2010; Ramanathan et al., 1997). However, these are limited to random microstructures and use statistical mechanical methods that use randomness in an essential manner. Furthermore, many of them use perturbative methods assuming small contrast. Recently, Srivastava et al. (2014) have studied the role of random inclusions on both toughness and roughness in ductile fracture.

* Corresponding author.

E-mail addresses: zubaer@caltech.edu (M.Z. Hossain), bourdin@lsu.edu (B. Bourdin), bhatta@caltech.edu (K. Bhattacharya).

Nature has exploited microstructure to enhance toughness of nacre and other shells. Various researchers have studied the underlying mechanisms and also sought to mimic the microstructure in bio-inspired designs (e.g. [Barthelat and Espinosa, 2007](#); [Currey and Taylor, 1974](#); [Evans et al., 2001](#); [Menig et al., 2000](#); [Nukala and Simunovic, 2005](#); [Begley et al., 2012](#)). Once again, this work is generally limited to particular classes of biologically relevant microstructures.

Through all of these works, there is an understanding that fracture toughness can be increased in a heterogeneous material by various mechanisms including crack deflection and meandering, zone shielding (through transformation toughening, microcrack toughening, crack-field void formation) and contact shielding (through wedging, bridging, sliding, plasticity induced crack-closure). Still, a comprehensive theory that describes the effective toughness of a heterogeneous medium is still to emerge.

There is a well-developed theory that describes the overall or effective properties of heterogeneous materials in the context of elasticity, electrostatics, magnetism and other properties that are characterized by variational principles, (e.g. [Milton, 2002](#); [Nemat-Nasser and Hori, 1999](#)). Many of these methods have been extended to dissipative processes like plasticity in the context of deformation theory or incremental update where one has a variational principle. Unfortunately, such a theoretical development remains missing in the case of fracture and other free-boundary/free-discontinuity problems. The key difficulty is that bounds on the energy do not necessarily imply bounds on the derivatives of the energy: a small bump in the energy landscape may become a very large bump in the forcing leading to changed behavior.

This is more than a theoretical difficulty, but points to the fact that in time-dependent or evolution problems, the effective macroscopic behavior can be very different from the underlying microscopic relations. In one dimension, it is known that a microscopically viscous evolution law can lead to a macroscopically stick-slip behavior ([Abeyaratne et al., 1996](#); [Bhattacharya, 1999](#)). Similar results have also been established for quasilinear free-boundary problems ([Dirr and Yip, 2006](#); [Dondl and Bhattacharya, 2014](#)). Recently, [Xia et al. \(2012, 2013\)](#) explored the role of heterogeneity in the mechanics of peeling adhesive tape. They showed that patterning the elastic stiffness of the tape (with no change in the actual adhesive) can lead to dramatically enhanced and possibly anisotropic and asymmetric resistance to peeling. All of these point to interesting phenomena in fracture.

The motivation for this work is three-fold. First, we seek a robust definition of effective toughness of an arbitrary heterogeneous media that is independent of macroscopic loading and with no *a priori* assumption or restriction about the evolution of the crack set at the microscopic scale. Second, we seek an approach to computing this effective toughness. Third, we seek insights into the relationship between microstructure and effective toughness. The emergence of new methods of synthesis – digital tools like rapid prototyping and ink-jet printing, and complex self-assembly – is creating an extraordinary new ability to synthesize materials and components with arbitrarily complex but precise microstructures. This presents a new opportunity to exploit a completely general class of precisely defined high contrast microstructures to design and synthesize materials and components that have a desired level of toughness.

We confine ourselves to brittle fracture for many reasons. First, brittle fracture provides a clear conceptual and theoretical framework to explore the main ideas. In contrast, ductile fracture brings other difficult issues including void formation. Second, catastrophic failure is a critical issue in brittle solids and affecting their toughness is technologically appealing. Finally, there is the recent work of [Srivastava et al. \(2014\)](#) in the ductile setting. We also confine ourselves to quasi-static evolution neglecting inertial effects for definiteness and simplicity since wave propagation in heterogeneous media is a complex issue in its own right. We confine ourselves to macroscopic Mode-I loading, again for definiteness and simplicity. We confine ourselves to propagation in a principal direction of the microstructure, and report on other directions elsewhere. Additionally, we confine ourselves to two dimensions (plane stress) and to periodic microstructures strictly for convenience. These may be relaxed at cost of complexity without affecting any of the ideas. Finally, we deliberately confine ourselves to the continuum scales. While atomistic effects are interesting in its own right (e.g., [Holland and Marder, 1998](#); [Kermode et al., 2008](#); [Freund, 2014](#)), the effect of heterogeneities on fracture properties as well as the synthesis techniques occurs at the neglected middle scales ranging from tens of nanometers to hundreds of microns that spans atoms to macroscopic continuum. Therefore, these scales provide an opportunity that has not been completely explored.

We begin in [Section 2](#) by proposing a definition of effective toughness, and then developing a numerical approach for computing it. Crack propagation depends sensitively on boundary conditions, but we seek a definition that is a material property and independent of the details of the boundary condition. Furthermore, our focus in this work is on macroscopically steady propagation. The key idea is what we call a *surfing boundary condition*. We recall some classical results from linear elastic fracture mechanics in [Section 3](#) which we use to supplement our computations. We verify our computational approach in [Section 4](#) in a homogeneous material. We consider a series of examples in [Sections 5–8](#). We conclude in [Section 9](#) by recalling the main results and with a discussion.

2. A computational approach to effective toughness

2.1. Homogeneous material

The notion of fracture toughness in a homogenous body goes back to [Griffith \(1921\)](#). Consider a body subjected to a certain loading with a smooth crack evolving smoothly with time. We define an elastic energy release rate or driving force acting on the crack front as the negative of the rate of change of the elastic potential energy U with crack length. We state

that the crack continues to grow if this energy release rate is equal to a critical value G_c :

$$G_c = -\frac{\partial U}{\partial a}. \quad (1)$$

The energy release rate is given by the celebrated path-independent J -integral (Cherepanov, 1967; Rice, 1968)

$$J = \int_c \hat{t} \cdot C \hat{n} dl \quad (2)$$

where \hat{n} is the outward normal to the contour \hat{t} is the tangent to the crack tip and

$$C = \varphi I - (\nabla u)^T \sigma \quad (3)$$

is Eshelby's energy-momentum tensor or the configurational stress tensor, $\varphi = \frac{1}{2} e(u) \cdot Ce(u)$ the elastic energy density, u the displacement, $e(u) = \frac{1}{2} (\nabla u + \nabla u^T)$ the strain and σ the Cauchy stress (in the linear elastic setting.) In a homogeneous material, the J -integral is path-independent since the energy-momentum tensor is divergence-free. One can also relate the J -integral to rate of dissipation of energy (Knowles, 1981) and the configurational force balance (Gurtin and Podio-Guidugli, 1996).

Finally, it is conventional in linear elastic fracture mechanics to perform an asymptotic expansion of the elastic field near the crack tip. For a Mode-I crack (where the crack is opened normal to the crack surface), the displacement fields (e.g., Zehnder, 2012) are given as

$$\begin{aligned} U_x &= \frac{K_I}{2\mu} \sqrt{\frac{r}{2\pi}} (\kappa - \cos \theta) \cos \frac{\theta}{2} \\ U_y &= \frac{K_I}{2\mu} \sqrt{\frac{r}{2\pi}} (\kappa - \cos \theta) \sin \frac{\theta}{2} \end{aligned} \quad (4)$$

K_I is called the stress-intensity factor, $\kappa = (3 - \nu)/(1 + \nu)$, $\mu = E/2(1 + \nu)$, and (r, θ) are polar co-ordinates emanating from the crack tip. It is conventional to describe the crack-propagation criterion as $K_I \geq K_{Ic}$ where K_{Ic} is known as the fracture toughness of the material. It is entirely equivalent to the considerations above, due to Irwin's relation (Irwin, 1957),

$$J = \frac{K_I^2}{E}. \quad (5)$$

With some abuse of terminology, we refer to $G_c = K_{Ic}^2/E$ as the toughness of the material.

The considerations above tell us about the propagation of an existing crack. An additional criterion is necessary for nucleation of cracks. A general formulation of this remains a topic of active research, but it is often specified as a length-scale that represents the size of a critical crack nucleus (Zehnder, 2012).

2.2. Heterogeneous materials: Surfing boundary conditions

The situation can be quite different in heterogeneous materials. First, cracks may not propagate smoothly with time. Instead it may be arrested at obstacles and then suddenly jump. Second, cracks may not propagate along a smooth path but may kink at interfaces and defects. Third, the J -integral is no longer path-independent. Fourth, crack branching and microcracking distant from the main crack may occur so that the notion of a crack itself may be poorly defined. Fifth, the state of stress can be extremely complex and asymptotic analysis may not be feasible. For these and other reasons, the study of fracture of heterogeneous media is a difficult subject.

We are interested in a situation where the scale of the heterogeneity is small compared to the scale of the domain or the boundary conditions, and we endeavor to describe a macroscopic propagation law. In other words, we seek to define an effective homogeneous medium with an effective elastic modulus and an effective fracture toughness that describes the results of a macroscopic experiment without having to resolve the microscopic details. This requires us to define a problem where one has steady and defined crack growth at the macroscopic scale, but where crack set is completely free to evolve in any manner that they choose at the microscopic scale.

We achieve this by solving the microscopic problem subject to what we call the *surfing boundary condition*. We consider a large domain Ω with periodic microstructure and subject it to a time-dependent steadily translating crack opening displacement. While the particular form we take is not important, for most of our calculations we take

$$u(x, y, t) = U(x - vt, y) \quad \text{on } \partial\Omega \quad (6)$$

where U is the Mode-I crack opening displacement (4) with a given K_I and the elastic modulus is taken to be the effective elastic modulus of the material. To verify that our definition and results are independent of boundary condition, we also consider on occasion the alternate boundary condition

$$u(x, y, t) = \left(\frac{A}{2} \left(1 - \tanh \left(\frac{x - vt}{d} \right) \right) \right) \text{sign}(y) \quad (7)$$

for constants A and d . Note that in each case, the boundary condition corresponds to a macroscopic crack propagating in the x -direction with constant imposed velocity v .

We then let the crack set evolve as it chooses, and compute the state of stress at each time. We compute the macroscopic energy release rate J at each time taking the boundary as the contour. After an initial transient stage, this $J(t)$ falls into a periodic pattern as long as the crack set is away from the boundary and define the maximum macroscopic energy release rate to be the *effective toughness*.

A few comments are in order. First, the goal of this formulation is to provide an effective toughness that is a material property independent of specific boundary conditions. Underlying our formulation is a conjectured homogenization result that such a quantity is indeed well defined and that our surfing boundary condition does compute it. Second, and related, is our conjecture that J -integral reaches a limiting value as the domain becomes infinitely large. Finally, note that we take the maximum value of the J -integral and not the average. This is because the effective toughness is characterized by the critical points in energy. We return to these issues in [Section 9](#).

2.3. Numerical solution to fracture mechanics

It remains to study the evolution of the crack set and the elastic fields at the microscopic scale within the domain Ω . We do so following a variant of the variational fracture field approach of Bourdin and collaborators ([Bourdin et al., 2000, 2008](#)). In this approach we introduce a scalar regularized fracture field $v(x, y, t)$ taking values in $[0, 1]$ and such that $v=0$ corresponds to a complete fracture and $v=1$ corresponds to an intact material. At the n th time step, we are given v^n , and we solve for fracture field v^{n+1} and the displacement field u^{n+1} as minimizers of the energy

$$U_{\text{total}} = \int_{\Omega} \left\{ \frac{1}{2} (v^2 + \eta) e(u) \cdot \mathbb{C}(x, y) e(u) + \frac{G_c(x, y)}{c_v} \left(\frac{1-v}{\varepsilon} + \varepsilon |\nabla v|^2 \right) \right\} dA, \quad (8)$$

$$U_{\text{total}} = U_{\text{elastic}} + U_{\text{fracture}} \quad (9)$$

where $c_v = \frac{8}{3}$ is a normalization constant, subject to the constraint $0 \leq v^{n+1} \leq v^n \leq 1$. Above, η, ε are small parameters, and \mathbb{C} and G_c are the pointwise elastic modulus and the fracture toughness respectively (we emphasize the heterogeneity in the material by explicitly noting their spatial dependence), and $e(u) = (\nabla u + \nabla u^T)/2$ is strain.

The minimizer has the property that $v=1$ everywhere except in small narrow regions of width $O(\varepsilon)$. These narrow regions can be interpreted as cracks. In fact, it can be shown rigorously following [Ambrosio and Tortorelli \(1990\)](#) that the energy above Gamma-converges to a sum of elastic and fracture energies as $\varepsilon \rightarrow 0$. Roughly, the minimizers of this energy (8) converges to the minimizers of the traditional energy

$$\int_{\Omega \setminus \Gamma} \frac{1}{2} e(u) \cdot \mathbb{C}(x, y) e(u) dA + \int_{\Gamma} G_c(x) dl \quad (10)$$

where Γ is an unknown crack set.

In other words, the regularized fracture field approach above may be viewed as an approximation (regularization) of the variational approach to fracture proposed by [Francfort and Marigo \(1998\)](#). This in turn is a natural extension of the ideas of Griffith that does not require *a priori* the restriction that cracks are smooth and they propagate smoothly. In short, the approach followed here provides an accurate numerical approximation to crack propagation with no *a priori* assumptions on the crack geometry or evolution. Furthermore, this approach is rate-independent.

An important clarification in understanding this regularized framework is that one should regard the crack as the strip of order ε where $v \neq 1$, instead of the surface where $v=0$. Then, one can show that the stresses at the edges of the strip have exactly the same properties as that of a sharp crack. Indeed, Gamma convergence implies that the displacements predicted by the regularized model agree (except in a region of order ε) with those of linear elastic fracture mechanics. This will be explicitly demonstrated in [Section 4](#).

The regularized theory introduces a length-scale through the regularization parameter ε . It has recently been shown that this length-scale sets the threshold for crack initiation, and therefore it can be argued that ε represents the crack initiation criterion ([Bourdin et al., 2014](#)).

We assume the fracture toughness to be isotropic and neglect interfacial effects. These are not limitations of the framework, and we explore these in ongoing work.

Note that the functional U_{total} is separately convex in u and v : so the problem of minimizing it in u for fixed v is well-posed, as is the problem of minimizing in v for fixed u . It is non-convex in (u, v) due to the first term $(v^2 \nabla u \cdot \mathbb{C} \nabla u)$. This is the reason that crack sets can spontaneously nucleate and jump. However, this makes it difficult to solve. So we solve the equations sequentially, and this leads to the Euler–Lagrange equation

$$\nabla \cdot ((v^2 + \eta) \mathbb{C} e(u)) = 0, \quad (11)$$

for the elastic equilibrium, while optimality with respect to v involves solving a constrained minimization problem. Both problems are implemented on a supercomputer using unstructured linear finite elements. The basic infrastructure for the

mesh management and parallel linear algebra is provided by PETSc (Balay et al., 2013a, 2013b, 1997), and the constrained optimization is based on TAO (Munson et al., 2012).

Following (Bourdin et al., 2008), we note that for a given regularization parameter ε and mesh size h , the fracture toughness is amplified by a factor

$$G_c^{\text{num}} = G_c \left(1 + \frac{h}{c_v \varepsilon} \right). \quad (12)$$

The effect is accounted for in our numerical simulation. We refer the reader to the above-mentioned references for further discussion.

Before we proceed, it is useful to non-dimensionalize the equations. We use a typical value of Young's modulus E_0 to set the energy scale, and a typical value of the length scale

$$L_0 = \frac{G_c}{E} = \left(\frac{K_{Ic}}{E} \right)^2. \quad (13)$$

to non-dimensionalize our equations. The model we use is rate-independent, and so only time-scale is given by the boundary condition, and so we regard that as non-dimensional. Specifically, we divide the total energy U_{total} in (8) by $E_0 L_0^3$ and set

$$\bar{\mathbb{C}} = \frac{\mathbb{C}}{E_0}, \quad \bar{G}_c = \frac{G_c}{E_0 L_0}, \quad \bar{\varepsilon} = \frac{\varepsilon}{L_0}, \quad \bar{\Omega} = \frac{1}{L_0} \Omega, \quad \bar{u} = \frac{u}{L_0}, \quad \bar{x} = \frac{x}{L_0}. \quad (14)$$

We obtain the same expression as (8) except each quantity is replaced by its non-dimensional counterpart (ν and η are already non-dimensional). So we drop the bar, and treat of the quantities in (8) as being non-dimensional.¹

We use the following non-dimensional values unless otherwise stated.

$$E = 1, \quad G_c = 1, \quad \nu = 0.2, \quad \varepsilon = 0.5, \quad h = 0.1, \quad K_I = 1.5 \quad (15)$$

Note that we have used the numerical discretization h to be much smaller than ε for convergence.

3. Semi-analytic method for small elastic contrast

We take a brief detour to recall some results of classical linear elastic fracture mechanics (see for example Zehnder, 2012; Gao, 1991 for further details). We will use these results to provide insight into the examples below by deriving semi-analytic solutions in the regime of small elastic contrast.

Consider an infinite body with elastic modulus $\mathbb{C}(x, y)$ and a semi-infinite crack $\Gamma = (-\infty, 0) \times \{0\}$ subjected to far-field Mode-I loading. We assume that the elastic contrast is small so that $\mathbb{C}(x, y) = \mathbb{C}^0 + \mathbb{C}^1(x, y)$ with \mathbb{C}^0 uniform and $|\mathbb{C}^1| \ll |\mathbb{C}^0|$. We obtain the solution to this problem asymptotically by making the ansatz that the elastic displacement field $u = u^0 + u^1$ with $|u^1| \ll |u^0|$. It follows that u^0 is the solution to the problem in the homogenous medium with modulus \mathbb{C}^0 and thus given by (4) for an isotropic elastic material. Furthermore, u^1 also satisfies a problem in the homogeneous medium with modulus \mathbb{C}^0 , but with an additional body force from the heterogeneity:

$$\mathbb{C}_{ijkl}^0 u_{k,lj}^1 = -(\mathbb{C}_{ijkl}^1 u_{k,l}^0)_{,j} =: -b_i. \quad (16)$$

We will be interested in situations where \mathbb{C}^1 is discontinuous and thus the derivative on the right-hand side has to be interpreted in the distributional sense. Specifically, if \mathbb{C}^1 is uniform and isotropic on Ω and zero outside, then one has a concentrated body force on the boundary of Ω and

$$b_i = - \int_{\Omega} \delta(x-y) (\lambda^1 \epsilon_{kk}^0 n_i + 2\mu^1 \epsilon_{ij}^0 n_j) dl_j \quad (17)$$

where n is the outward normal to Ω .

We solve (16) by superposition of (i) a body with no crack but subjected to the given body force and (ii) a body with a crack whose crack faces are subject to the tractions equal and opposite to those inferred from problem (i). We solve problem (i) using Papkovitch–Neuber–Boussinesq potentials to obtain

$$u^1 = \frac{1}{2\mu} (\nabla(\phi + x \cdot \psi) - 4(1-\nu)\psi) \quad (18)$$

where ϕ and ψ satisfy Poisson's equations

$$\Delta\phi = -\frac{1}{2(1-\nu)} b \cdot x, \quad \Delta\psi = \frac{1}{2(1-\nu)} b \quad (19)$$

¹ Note that this scaling is different from what is typically used in fracture mechanics of homogeneous materials. Typically, the displacement is scaled by $\sqrt{G_c L/E}$ where L is the size of the domain. This makes the elastic and fracture energies in (10) comparable, and thereby renders fracture parameter-independent. However, this typical scaling is not effective in our problem since we consider heterogeneous materials and since we use a regularized theory.

that are solved using the fundamental solution ($\log |x|$ in two dimensions). We then obtain the stress field σ^{1i} and the tractions t^\pm that they impose on the location of the crack faces (\pm denotes the two crack faces).

We solve problem (ii) using the Bueckner weight function (Bueckner, 1970). Define the complex function $R = (t_n - it_s)$ where t_n and t_s are the normal and shear components of the traction on the $+$ crack face. Then, complex stress intensity factor $K^* = \sqrt{\pi}(K_I - iK_{II})$ due to the perturbed field is given by

$$K^* = \frac{\sqrt{2}}{\pi} \int_{-\infty}^0 R(t)|t|^{-1/2} dt. \quad (20)$$

4. Verification on homogeneous materials

A typical result of a simulation on a homogeneous material is shown in Fig. 1. We consider a square domain of size 65×48 with an initial crack of length 10 (Fig. 1(a)). We apply the surfing boundary conditions (6) with $K_I=1.0$, and $G_c=1.5$. The rest of the parameters are as in (15). The computed horizontal displacement field u_x at $t=0^+$ is shown in Fig. 1(b) and (c) along the x - and y -axis respectively, with the origin located at the crack tip. Note that they agree very well with the analytic K_I field (4), except close to the crack tip due to the regularization. The computed J -integral along the boundary as well as the position of the crack are shown in Fig. 1(d). Note that the initial J is very close to the expected value $K_I^2/E=1$; it is slightly smaller because of the regularization at the crack tip. Since this J is lower than the G_c for the material, the crack does not grow. As time progresses and the applied opening displacement translates to the right, the value of J at the boundary increases. The crack begins to grow as soon as J reaches the value $G_c^{\text{num}}=1.6$ and then grows steadily with the velocity of the imposed boundary condition as J remains constant. Thus, the critical J inferred from the boundary conditions when the crack propagates steadily is in fact equal to the toughness of the material.

Fig. 2(a,b) shows the results of the same computation as above but with various values of G_c . Notice from Fig. 2(a) that, in each case, the critical J inferred from the boundary conditions when the crack propagates steadily is in fact equal to the toughness G_c^{num} of the material. Fig. 2(b) shows the fracture energy U_{fracture} (cf (9)), normalized with G_c , as a function of the crack length. The slope of this curve is exactly equal to G_c^{num} as we would expect in a homogeneous material. Fig. 2(c) shows the results of the same computation as above but with various values of applied K_I (holding $G_c=1.5$ fixed). Notice that while the initial value of J reflects the applied K_I , the critical value is independent of it. Finally, Fig. 2(d) shows the results of the computation with the alternate boundary condition (7) with $G_c=1.5$. In this case the transient creates a higher J , but it quickly reaches the steady value of $G_c^{\text{num}}=1.6$. So, the computed G_c is independent of the boundary condition.

Recall that when the applied K_I is lower than that corresponding to the material G_c , the crack tip trails the center of the applied boundary condition (Fig. 1(d)). We study this offset in Fig. 3. Fig. 3(b) shows the horizontal displacement field along

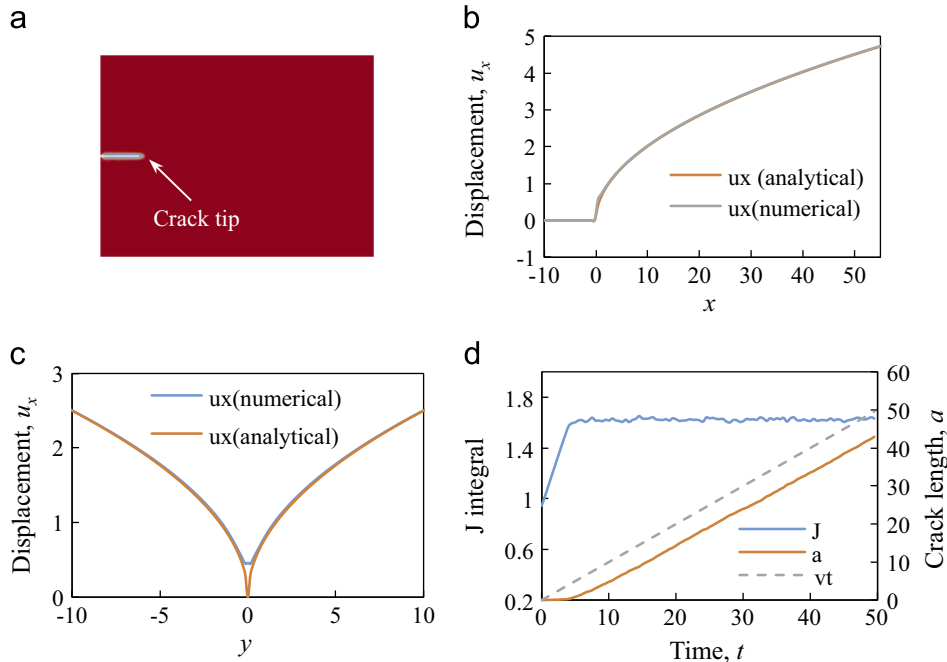


Fig. 1. Result of a typical simulation on a homogeneous material. (a) The initial configuration, (b,c) the computed horizontal displacement field u_x at $t=0^+$ along the x - and y - axis with the origin located at the crack tip and (d) the computed J integral on the boundary and crack length vs. time.

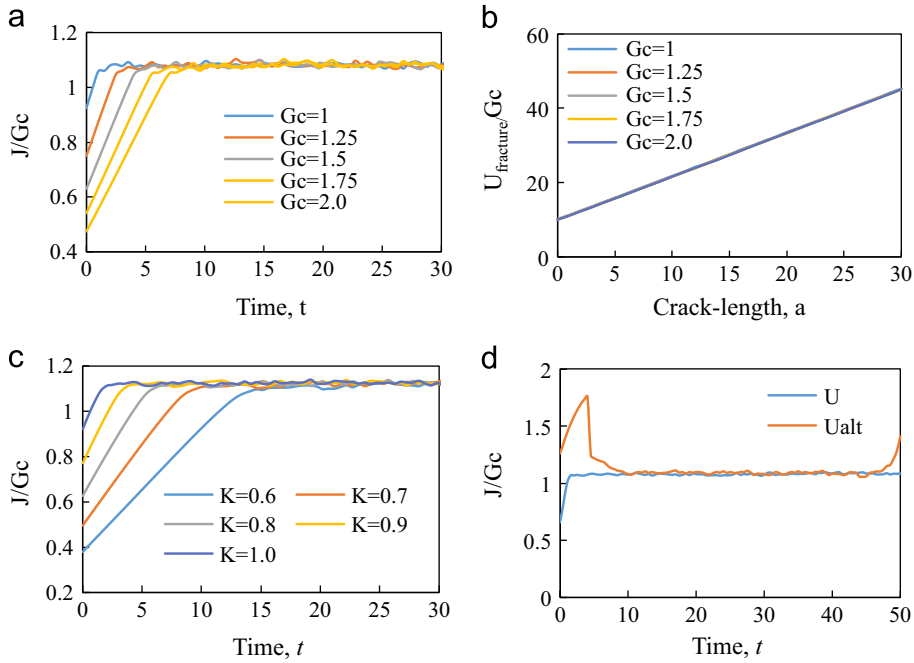


Fig. 2. Parameter study on a homogeneous material. (a) The computed J vs. time, (b) fracture energy vs. crack length for various values of G_c holding applied $K_I=1$ fixed, (c) the computed J vs. time for various values of applied K_I , holding $G_c=1.5$ fixed and (d) the computed J vs. time for the usual (U) and alternate boundary condition (U_{alt}) with $G_c=1.0$.

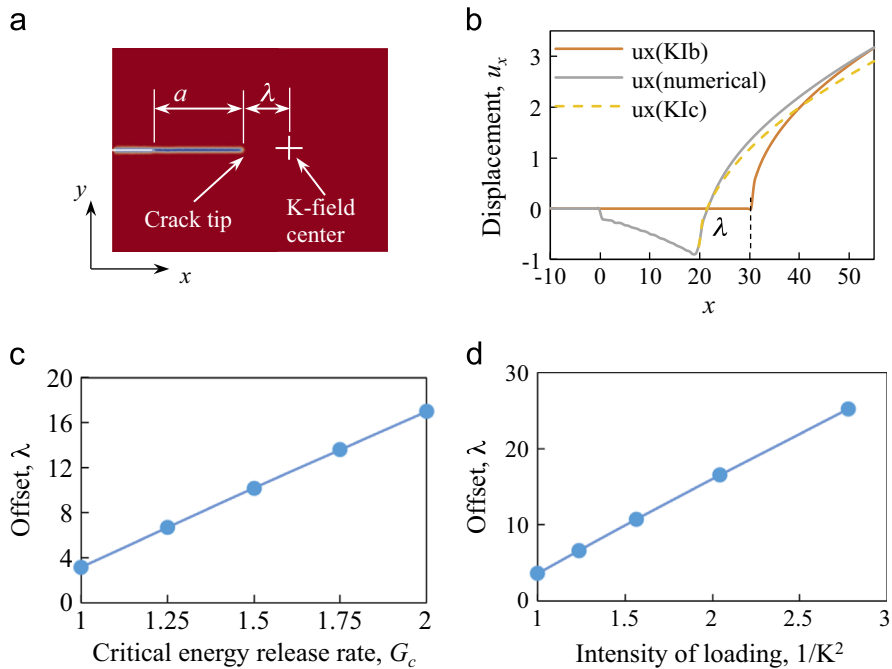


Fig. 3. (a) Offset between the crack tip and the center of the applied boundary condition, (b) displacement, (c) the computed offset for various G_c holding applied $K_I=1.0$ fixed and (d) the computed offset for various applied K_I holding $G_c=1.0$ fixed.

the x -axis with the original crack tip as the origin. Note that the displacement field is similar to that corresponding to K_{Ic} near the crack tip, but changes in the far field to that corresponding to the applied boundary value. Fig. 3(c) and (d) shows that the offset is proportional to G_c for fixed applied K_I , and inversely proportional to the square of the applied K_I for a fixed G_c . These relations are as expected from linear elastic fracture mechanics.

Putting all these together, we conclude that the surfing boundary conditions and the computational method provide the expected results in a homogeneous material.

5. Toughening due to elastic heterogeneity

In this section, we study two examples that show that elastic heterogeneity is a toughening mechanism. The first involves smooth modulation and was studied by Gao (1991) in the low contrast regime, and also provides a verification of the numerical method for heterogeneous media.

5.1. Smooth modulation: verification on heterogeneous materials

We now consider a domain with Young's modulus smoothly varying in the x -direction

$$E(x) = E_0 - E_A \cos\left(\frac{2\pi x}{\lambda}\right). \quad (21)$$

Poisson's ratio and the fracture toughness are kept uniform at $\nu=0.2$ and $G_c=1$. For computational efficiency, and also due to subtle point regarding the J -integral which we discuss later, we keep the microstructure in the core of the domain and surround it by a material with a homogeneous elastic region with elastic modulus equal to the effective modulus of the heterogeneous medium as shown in Fig. 4(a). We introduce a crack as shown, and apply a surfing boundary condition with $K_I=1.5$. We find that the crack propagates smoothly along a straight line ($y=0$). The computed J at the boundary (normalized by G_c^{num}) for two values of ϵ is shown in Fig. 4(b).

We find that the macroscopic J increases as the crack reaches the compliant region and then decreases as the crack reaches the stiff region. Briefly, the state of stress is heterogeneous and it is low in the regions with low elastic modulus. Therefore, we require a larger driving force to propagate the crack through this region. Importantly, the crack has to reach a macroscopic value that is 1.10 times higher than the uniform pointwise value before it can propagate through a macroscopic distance. Therefore, the *macroscopic effective toughness is higher than the uniform pointwise toughness of the medium*. Furthermore, the crack path remains straight in this example so that this higher value has little to do with crack deviation. Therefore we conclude that elastic heterogeneity is in itself a toughening mechanism. Finally, since the crack propagation is smooth and there is no instability or re-nucleation involved, the computed J is independent of the value of ϵ as shown.

We have verified that the computed J on the boundary is independent of the constant K_I in the surfing boundary condition. As shown in Fig. 2(c) for the homogeneous case, the time when the crack begins to propagate changes with the constant K_I in the boundary condition, but not the driving force at which it begins propagation.

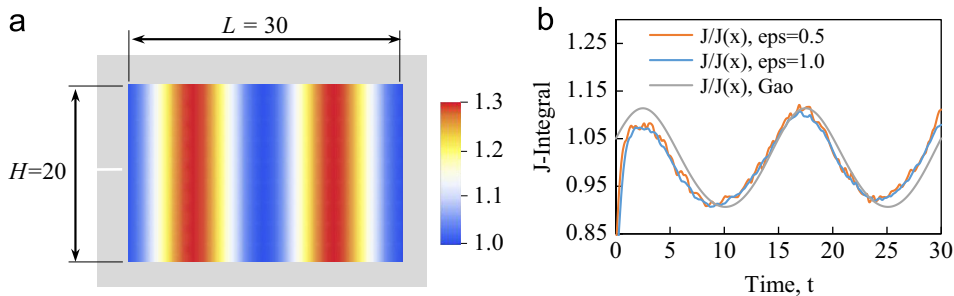


Fig. 4. Example showing toughening due to elastic heterogeneity and verification of the proposed method. (a) Computation domain with elastic modulus sinusoidally varying in the x -direction from $E_{\min} = 1$ to $E_{\max} = 1.3$ (with $E_0 = 1.15$, $E_A = 0.15$, $\lambda = 15$), but uniform toughness $G_c = 1$ and (b) computed J and crack length vs. time for two values of ϵ as well as the analytic solution of Gao (1991).

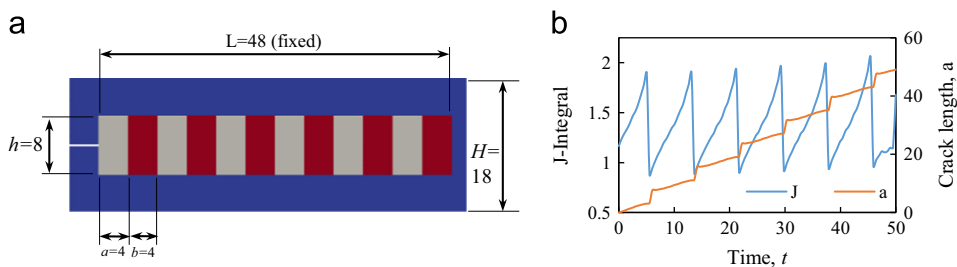


Fig. 5. Simple example showing toughening due to elastic heterogeneity: stripes with alternating elastic modulus $E = 1$ and $E = 2$, but uniform toughness $G_c = 1$. (a) Computational region and (b) computed J and crack length vs. time, with $\epsilon = 0.25$, $h = 0.1$.

Gao (1991) had studied this problem in the low contrast regime described in Section 3. Using similar techniques he has shown that

$$\frac{K(x)}{K_\infty} = 1 + \frac{3-4\nu}{8(1-\nu)} \frac{E_A}{E_\infty} \left(2 \cos\left(\frac{2\pi x}{\lambda} + \pi\right) + \sin\left(\frac{2\pi x}{\lambda} + \pi\right) \right) \quad (22)$$

where $K(x)$ is the stress-intensity factor at the crack-tip when it is at the position x and K_∞ is the macroscopic stress-intensity factor. We can use Irwin's formula (5) (separately at the tip and at infinity) to obtain the ratio of the crack-tip energy release rate $J^{\text{tip}}(x)$ to the macroscopic energy release rate J . Using the crack propagation criterion $J^{\text{tip}}(x) = G_c$ gives us the value of the macroscopic energy release rate J when the crack-tip is at the point x . This is also shown in Fig. 4(b). We find good agreement, thereby verifying our computation approach to computing effective toughness.

5.2. Layered materials

We now consider a layered material with alternating stiffness of $E=2$ and $E=1$ as shown in Fig. 5. The stripes have equal areal fraction and are of width 2 (or period 4). The Poisson ratio is uniform at 0.2, and importantly the toughness is uniform at $G_c=1$. Finally $\varepsilon=0.25$. For computational efficiency, and also due to subtle point regarding the J -integral which we discuss later, we keep the microstructure in the core of the domain (48×8) and surround it by a material with a homogeneous elastic region with elastic modulus equal to the effective modulus of the heterogeneous medium.

We introduce a crack of length 5 as before and apply a surfing boundary condition with $K_I=1.5$. We observe that the crack does not propagate smoothly. Instead, it gets trapped in the compliant layer (before the interface separating the compliant and stiff layers) and the computed J on the boundary begins to rise. The crack eventually breaks through when J reaches a critical value and jumps across the interface and bulk of the stiff material. This is accompanied with a drop in J . The crack then grows slowly and smoothly for a short distance before getting trapped once again. Moreover, the crack path remains straight.

The important observation here is that the applied J has to reach a value 1.91 before the crack can propagate through a macroscopic distance.² Thus, the effective toughness is characterized by $G_c^{\text{eff}} = 1.91$. Note that this is strictly larger than the uniform toughness of the medium $G_c^{\text{num}} = 1.15$. Furthermore, the crack path remains straight and we again conclude that elastic heterogeneity is in itself a toughening mechanism.

Fig. 6 shows further details of the example. Fig. 6(a,b) shows the total elastic and fracture energy as a function of time and as a function of crack length respectively. Notice that the elastic energy builds up as the crack is trapped and is suddenly released when the crack jumps. The fracture energy does exactly the opposite. The total energy also shows oscillations. Fig. 6(c) shows the effect of ε (the regularization parameter) keeping h/ε fixed. Notice that this value increases with decreasing ε . We will discuss this dependence presently. Fig. 6(d) shows the results of the computation with domains of various sizes. We find that the result is essentially independent of the domain size. We have also verified the independence with respect to boundary condition by repeating the calculation with various applied K_I as well as the alternate boundary condition (7).

There are two reasons for the toughening. First, in the absence of the crack, the compliant region has a lower value of stress than the stiff region. Therefore, if the width of the stripes is large enough, the crack tip experiences a lower driving force when it is in the compliant region. Therefore the macroscopic driving force has to be increased to propagate it through this region. A simple calculation shows that this would lead to an increase in G_c^{eff} exactly equal to the ratio of the effective Young's modulus to that of the compliant material. In our example this would mean $G_c^{\text{contrast}} = 1.5$ so that $G_c^{\text{contrast,num}} = 1.725$, but this is lower than what we observe.

This points to the second reason. As the crack approaches the stiff region from the compliant region, some of the driving force on the boundary is consumed in suddenly deforming the stiff region. Thus, continued propagation of the crack requires even higher macroscopic driving force. We examine this second reason qualitatively in Fig. 7 using the semi-analytic method. Consider an infinite domain, with a semi-infinite crack approaching the interface between a compliant region (left) and a stiff region (right) as shown in Fig. 7(a). As the crack approaches the interface, we see that the crack intensity factor and the driving force on the crack front decreases as shown in Fig. 7(b). Thus sustained propagation requires increased driving force.

Note that the K_I diverges as the crack-tip approaches the interface, as noted by Atkinson (1975). In fact, Zak and Williams (1963) showed that when the crack tip is at the interface going from a compliant to a stiff material, the stress field at the crack-tip is not singular and so that the stress-intensity factor is zero. Thus the crack is arrested at this interface and has to re-nucleate. This depends critically on the crack-initiation criterion and thus depends on the value of ε .

We repeat the calculation for various values of parameters (for $\varepsilon=0.25$, $h=0.1$ fixed) and show the results in Fig. 8. Fig. 8(a) shows how the effective toughness varies with elastic contrast. As the contrast increases, so does the effective toughness due to the contrast in state of stress. Fig. 8(b) shows the effective toughness for various values of the strip width holding the elastic contrast at 2. Notice that the toughness increases with strip width saturating at 1.91 but decreases to the uniform microscopic value of 1.15 with decreasing length-scale. To understand this, notice that our regularized model has a length-scale due to ε . If the scale of the heterogeneity is small compared to this length-scale, the crack tip sees a uniform

² We take the average of the first three peaks since one has end effects on the subsequent ones.

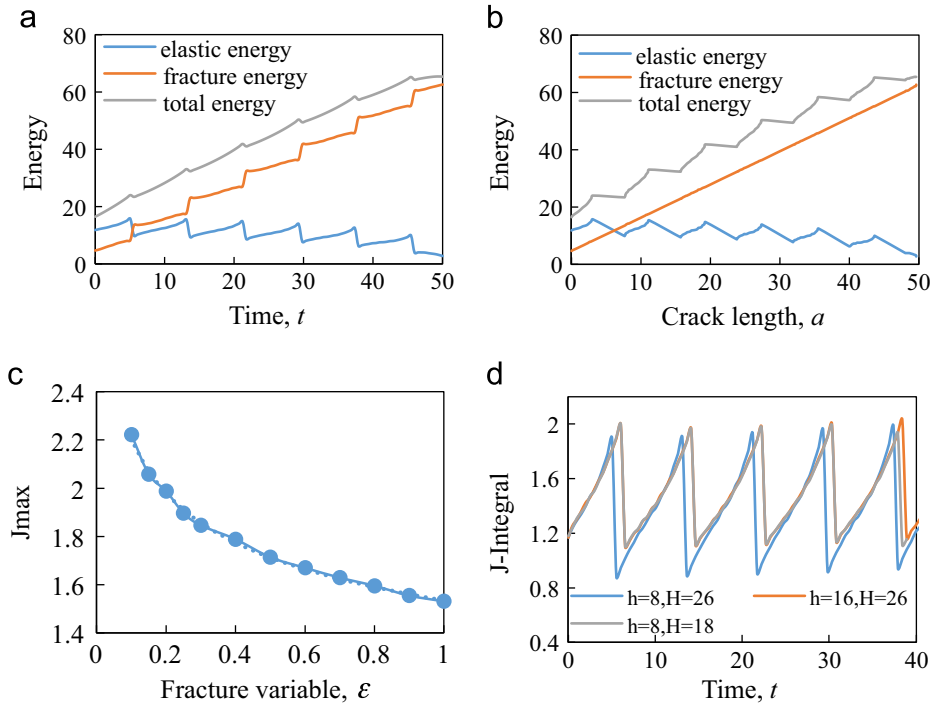


Fig. 6. (a, b) Energy vs. time and crack length for the crack propagating in the stripe domain shown in Fig. 5, (c) the computed peak J for various ϵ holding $h/\epsilon = 0.2$ fixed and (d) the computed peak J for various domains with $\epsilon = 0.25$, $h = 0.1$.

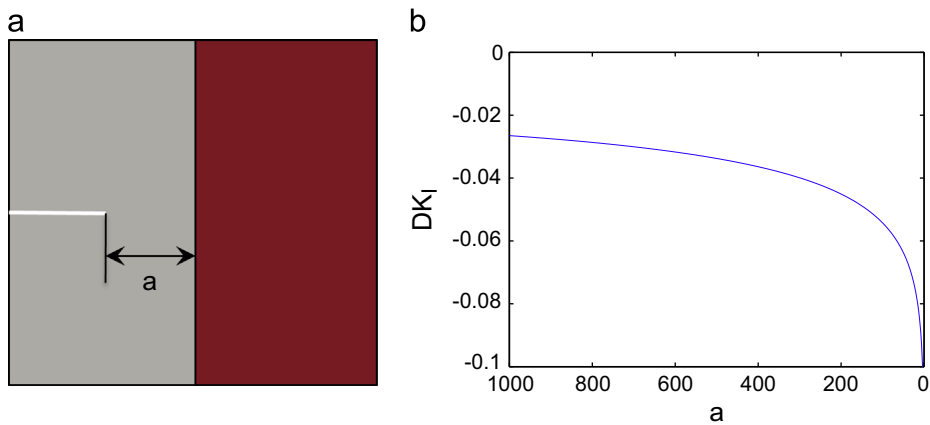


Fig. 7. Semi-analytic study of a crack approaching an interface with a stiffer material in an infinite domain. (a) Domain and (b) the change in K_I at the crack tip with distance between the crack tip and the interface.

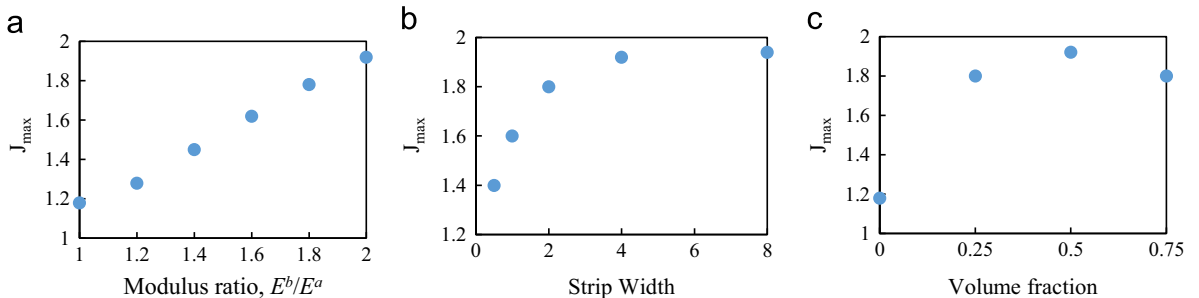


Fig. 8. Parameter study of the effective toughness of the stripes with elastic heterogeneity with respect to (a) elastic contrast, (b) strip width and (c) volume fraction, with $\epsilon = 0.25$, $h = 0.1$.

elastic material. Since the toughness is uniform in our case, it behaves as if it is in a homogeneous medium and there is no toughening. Fig. 8(c) shows that volume fraction has some effect, but this is related to length-scales. In these calculations, the period is held fixed at 4, and so the width of one material or the other becomes small when the volume fraction approaches 0 or 1.

Before we proceed, we make one final comment about this example. Since the continued propagation is dictated by re-initiation of the crack once it reaches the interface, the interfacial toughness plays an important role. Indeed He and Hutchinson (1989) showed that the crack can deflect into the interface if the interfacial toughness is small enough. We do not observe the deflection here since the interfacial toughness is exactly the same as the bulk toughness. We are currently using the framework proposed in this paper to study situations with weak interfaces.

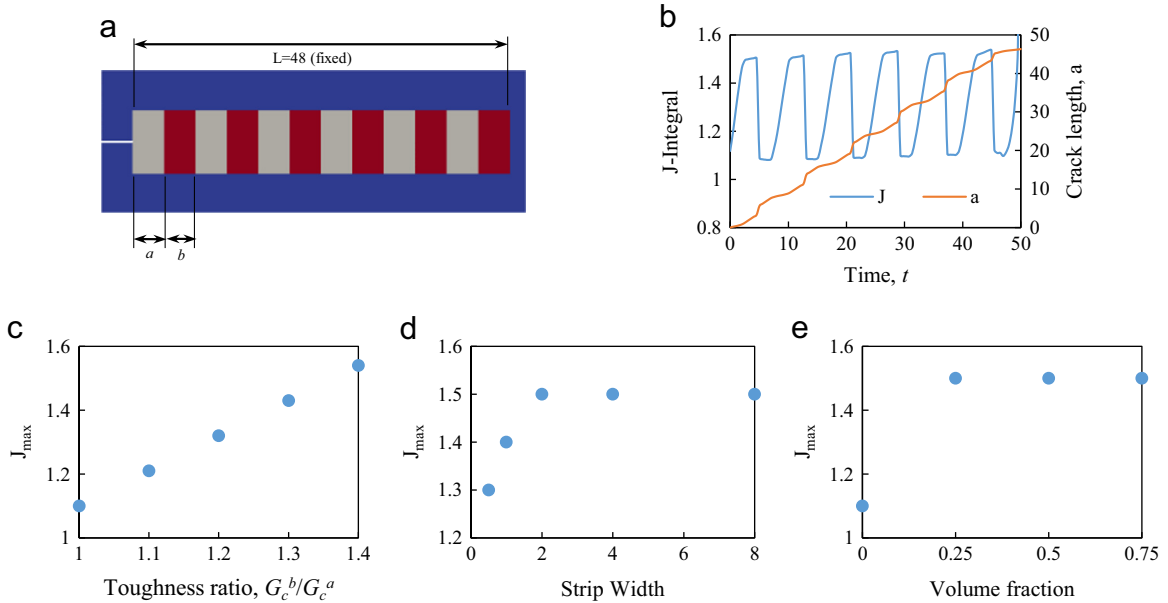


Fig. 9. Simple example showing toughening due to toughness heterogeneity: stripes with alternating elastic toughness, and $\epsilon=0.25$, $h=0.1$. (a) Computational region, (b) computed J and crack length vs. time when $G_c=1$ and $G_c=1.5$ and uniform modulus $E=1$ and (c–e) parameter study of the effective toughness vs. toughness contrast with $G_c^a=1$ (c), strip width (d) and volume fraction (e).

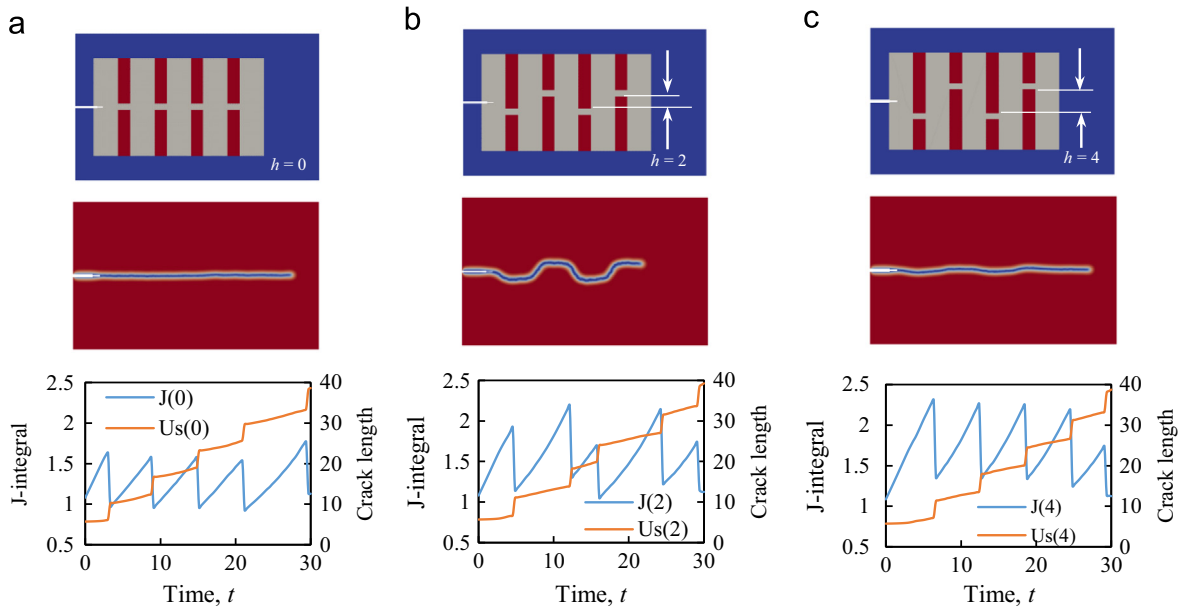


Fig. 10. Elastic heterogeneity with broken stripes where the stripe of the stiff material has a gap through which the compliant material percolates. The gaps are aligned in (a), but misaligned by 2 in (b) and 4 in (c). The top figure of each column shows the domain, the middle image shows the computed crack path and the bottom shows a plot of the computed J and crack length vs. time.

6. Toughening due to toughness heterogeneity

We study the complementary situation of a stripe domain with uniform elastic modulus but alternating toughness in this section. The results are shown in Fig. 9. Since the elastic modulus is uniform, the J integral is path independent and thus, the applied stress intensity is equal to the stress intensity at the crack tip. Hence, the crack propagates when and only when the macroscopic J is equal to the value of G_c at the crack-tip. Thus we expect the applied J to alternate between two values of G_c^{num} . This is exactly what we see in Fig. 9(b). Further we see that the crack is trapped at the interface between the low and high toughness stripes before jumping through. Finally, the crack can propagate through macroscopic distances only when the applied J reaches the larger of the two values. Consequently the effective toughness is equal to the larger – and not the average – of the two values of G_c^{num} . Importantly, *the effective toughness is different from the average surface energy*. Fig. 9(c–e) show a parameter study. G_c^{eff} is always equal to the larger of the two G_c . The effective toughness is independent of the strip width and the volume fraction – it falls at small length-scales and volume fraction because our regularized model fails to see the heterogeneity when the scale of the heterogeneity becomes smaller than ε .

7. Toughening due to tortuosity

We now turn to an example where the crack is not necessarily straight. The microstructure is a variation on the theme of alternating stripes where the stiff layers are broken by a gap of compliant material as shown in Fig. 10. Young's moduli are taken to be 1 and 4, the width of each layer is 2 and the break in the stiff layer has height 1. The fracture toughness is taken to be uniform at $G_c=1$. The gaps in the different layers are either aligned as shown on the left column of the figure or staggered as shown in the middle and right columns.

When the gaps are all aligned, the crack propagates straight through the gaps. Still the applied J is not constant because the elastic fields are heterogeneous. Once again, the crack is trapped as it approaches the stiff stripes and discontinuously advances through the gaps. Furthermore, the effective toughness $G_c^{\text{eff}} = 1.6$ is strictly higher than the uniform microscopic $G_c=1$.

When the gaps are moderately misaligned as shown in middle column of Fig. 10, the crack meanders back and forth in a discontinuous manner to take advantage of the gaps. The macroscopic J is not uniform and the effective toughness $G_c^{\text{eff}} = 2.3$ is strictly higher than the uniform microscopic $G_c=1$. Note that in this example, the overall crack length is larger than in the case (a).³ This increased crack length would suggest a toughness of 1.5 which is lower than the computed number. Once again, effective toughness is higher than the effective surface area.

As the offset between the gaps increase beyond a certain point, the crack no longer meanders, but propagates straight in a jerky manner as if were passing through a layered material as shown in the third column of Fig. 10. The effective toughness is also similar to that of a layered material.

Fig. 11(a) shows how the effective toughness changes with the misalignment in the gaps. We see that it starts at a value greater than the pointwise toughness as discussed above when all the gaps are aligned, and increases with misalignment as the cracks meander to take advantage of the gaps. At some point ($h=3$ here), the toughness reaches the value that it would have if the material had no gaps; beyond that the crack propagates straight and the effective toughness saturates. Fig. 11(b) shows the effect of elastic contrast when the gap is held fixed at $h=4$. At small contrast, the crack propagates straight but meanders at large contrast.

8. Asymmetric fracture toughness

In this section, we present examples to show that the effective toughness can be asymmetric. It has long been understood that the toughness of composite media can be anisotropic, i.e., the toughness can depend on the direction of propagation of the crack. We now show that it can in fact be asymmetric in that the toughness depends on the sense of propagation. The key idea is that the state of stress at the crack tip depends not only on the location of the crack-tip and the tangent to the crack at the tip, but also on the position of the entire crack set.

The first example is shown in Fig. 12 and consists of stripes with a periodic, but asymmetric, distribution of elastic moduli. In Fig. 12(a), the modulus rises in four gradual steps before dropping rapidly while the pattern is inverted in Fig. 12 (b). In other words, the two figures show the same asymmetric geometry, but flipped horizontally with respect to each other. The toughness is taken to be uniform. A crack introduced on the left of each geometry and driven to the right. Therefore, the two columns depict the crack being driven in opposite sense relative to the pattern. In both cases the crack propagates straight. However, the computed J for the two case are quite different and not related by symmetry. In particular, the effective toughness is different in the two directions. To understand this, recall that the effective toughness in our previous example of stripes with alternating elastic moduli depends on the elastic contrast. In this example, the contrast going in one direction is different from that in the other direction. In short, *effective toughness can be asymmetric*. Fig. 12(c) put the two modulations together in two halves, and we see that the two halves have different effective toughness. Fig. 13

³ Though the bottom row shows that the crack length is the same at the end of the simulation in Fig. 10(a) and (b), the crack has traveled a great macroscopic distance in (a).

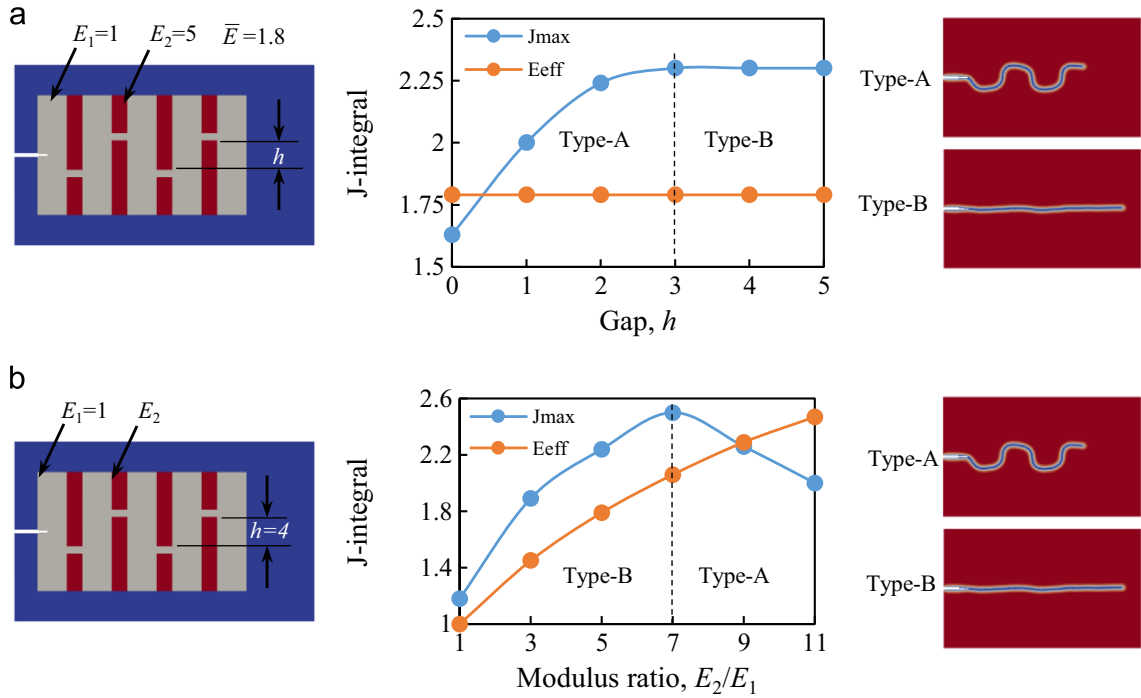


Fig. 11. Elastic heterogeneity with broken strips. Effective toughness vs. (a) misalignment of gap and (b) elastic contrast.

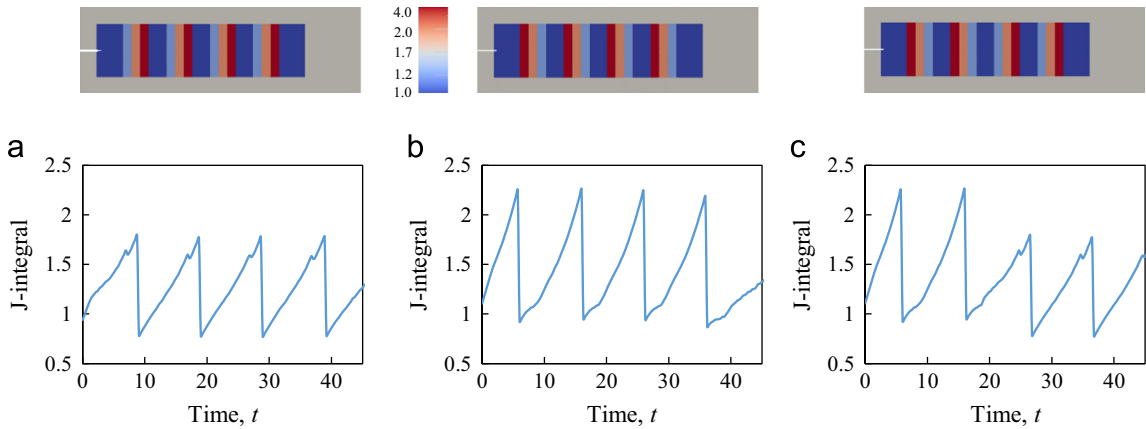


Fig. 12. Simple example showing that the fracture toughness can be asymmetric involving periodic pattern of stripes. (a) Elastic modulus gradually increases and then drops rapidly, (b) inverted pattern of (a), and (c) a combination of previous cases where the first half is as in (b) and the second as in (a). The toughness is uniform.

repeats the example with increased strip width to find increased contrast. We expect the asymmetry to vanish as the length-scale decreases to the inherent length-scale of fracture, and to increase with increasing length-scale with an eventual saturation.

The second example is shown in Fig. 14 and consists of asymmetric inclusions in a matrix. The toughness is again homogeneous. Fig. 14(a) shows the computational domain in two orientations. Fig. 14(b) shows the computed J vs. time as the crack propagates through the domain with compliant inclusions in a stiff matrix in two directions. The effective toughness is asymmetric. Fig. 14(c) shows the case of a domain with stiff inclusions in a compliant matrix. The effective toughness is asymmetric, but less than before. Fig. 15 shows that the computed results do not change if the initial crack is offset from the pattern, or if one has multiple rows of pattern so that the computed effective toughness represents a material rather than a structural property.

We supplement the simulations above with semi-analytic calculations. The method has difficulty when the crack-tip touches the heterogeneity. So we consider a variant where the crack propagates between a symmetric row of inclusions as shown in Fig. 16. Once again, we run the crack in two opposite directions relative to the asymmetric pattern, and see that there is a contrast in the resulting stress-intensity factor at the crack tip. We varied the shape of the two curved region using

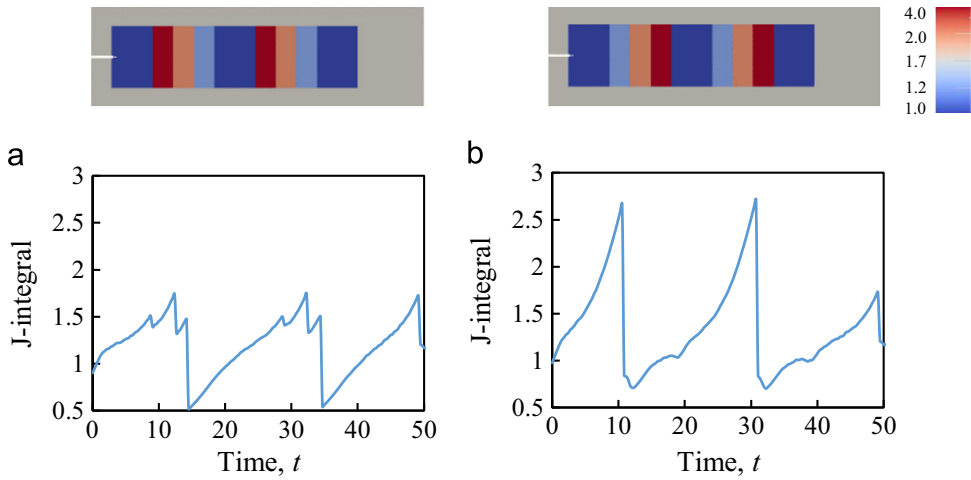


Fig. 13. Simple example showing that the fracture toughness can be asymmetric involving periodic pattern of stripes. Same as in Fig. 12(a,b) but with increased width.

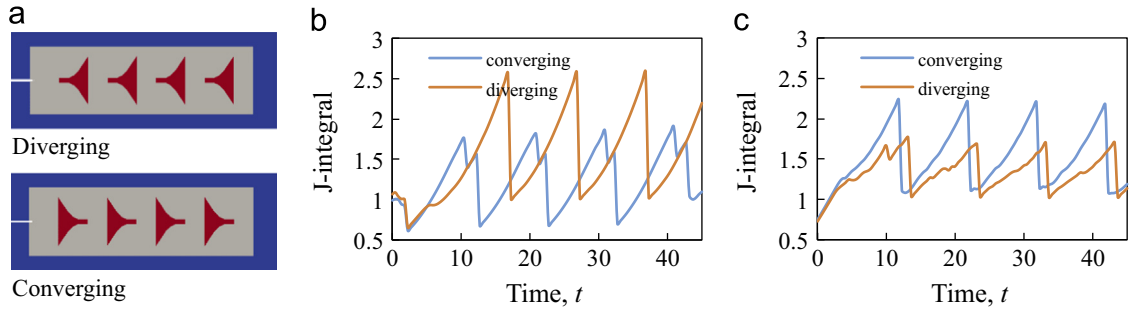


Fig. 14. Toughness asymmetry in a particulate material. (a) Domain (with size 55×20) with asymmetric inclusions in two orientations and (b,c) Computed J vs. time in the two orientations for the case of compliant inclusion in a stiff matrix(b) and for the case of stiff inclusions in a compliant matrix (c).

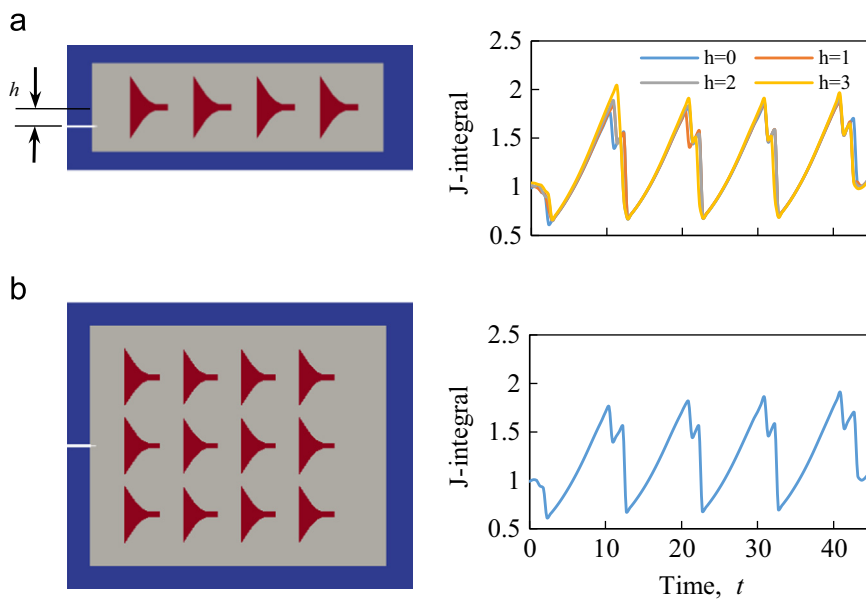


Fig. 15. The same example as in Fig. 14, but with the initial crack offset (a) and with three rows of inclusion (b).

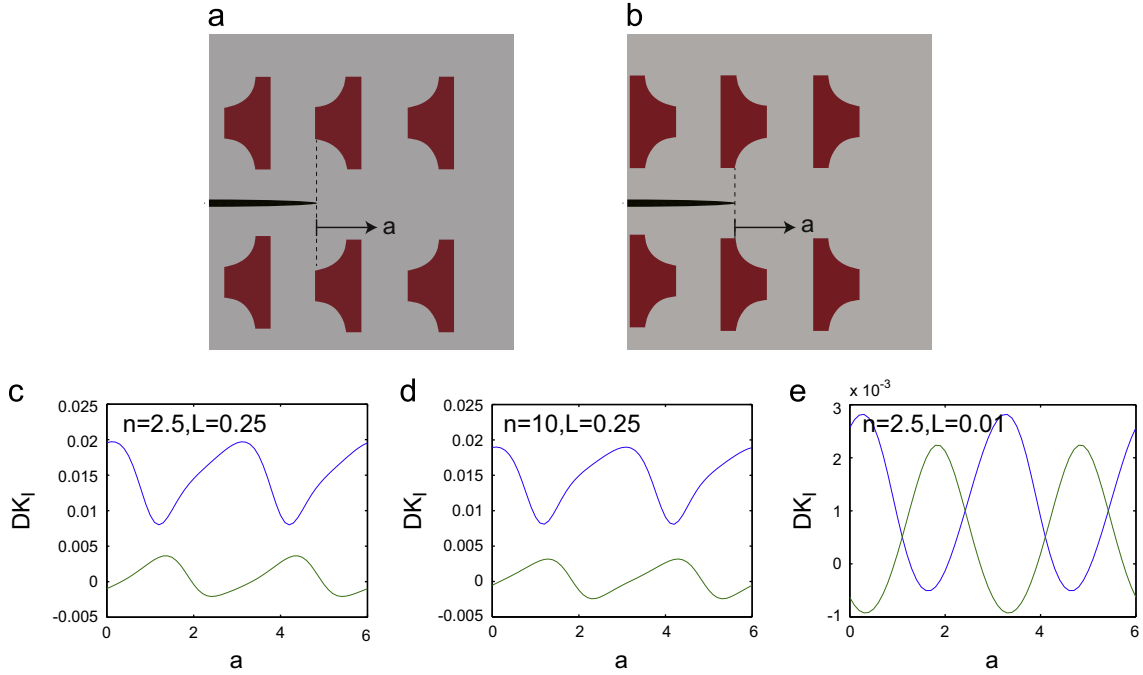


Fig. 16. Results of the semi-analytic calculations. (a,b) Asymmetric inclusions with crack propagating in opposite directions and (c–e) the change in stress-intensity factor as a result of the inclusions for a crack propagating as in (a) in blue and for a crack propagating as in (b) in green. (For interpretation of the references to color in this figure caption, the reader is referred to the web version of this article.)

various polynomial curves of the form $y = \pm (x - c_1)^n + c_0$ for various powers n , but this has little effect as shown in Fig. 16(c, d) for $n=2.5$ and $n=10$. We find however, that the width of the fat portion has an important effect as shown in Fig. 16(c,e) for $L=0.25$ and $L=0.01$.

These examples exploit the elastic heterogeneity and the fact that the state of stress is nonlocal, and thus depends on the entire crack set. We emphasize this by noting that we have modified these examples by making the elastic moduli uniform but the fracture toughness heterogeneous in an asymmetric manner. We see no asymmetry since the effective toughness in both directions is determined by the maximum value of the pointwise toughness.

9. Conclusion and discussion

In this paper, we have proposed a definition for the effective toughness of a heterogeneous media that is a material property independent of the details of the boundary condition. We have also proposed an approach to numerically computing this effective toughness. The key idea is what we call a surfing boundary condition. We consider a domain that is large compared to the heterogeneities, apply a displacement boundary condition that corresponds to a steadily propagating macroscopic crack and allow the crack set to evolve in any manner it chooses – steadily, discontinuously, meandering, branching, with microcrack nucleation, etc. – at the microscopic scale. We then define the effective toughness to be the macroscopic energy release rate that is required at the boundary to propagate the crack over a macroscopic distance. We verify the approach on homogeneous materials, and then use it to study a series of examples to explore various ideas.

Elastic heterogeneity: An important idea that we demonstrate and exploit is that elastic heterogeneity can have a profound effect on the fracture process. Specifically heterogeneous elastic modulus can lead to extremely large fluctuations in the state of stress. It follows then that the driving force on the crack tip is also extremely heterogeneous. This has been discussed earlier in the perturbative regime (Gao, 1991), but we show in this work that the effect is significant and the consequences can be manifold.

First, *elastic heterogeneity can be a toughening mechanism:* We demonstrate this in Section 5 with two examples of where Young's modulus varies in one direction and where a Mode-I crack is driven perpendicular to the variation. The crack path remains straight, but the overall toughness can be dramatically enhanced. This enhancement goes beyond fluctuations in stress and is supplemented by the shielding from interfaces. Furthermore, elastic heterogeneity can also lead to crack meandering as we demonstrate in Section 7, and this can further affect the toughening. We believe that elastic heterogeneity is indeed an important, but often overlooked, mechanism for toughening in ceramics. The anisotropy in elastic modulus of a single crystal manifests itself as elastic heterogeneity in the ceramic.

Second, *elastic heterogeneity can lead to an asymmetry in fracture toughness.* It has long been recognized that the toughness of a heterogeneous medium can be anisotropic. In Section 8, we demonstrate that the toughness can also depend

on the sense of propagation; a crack propagating in one direction is different from that propagating in the opposite. This asymmetry is a consequence of the fact that elasticity is non-local and thus the state of stress depends not only on the position of the crack tip but also on the location of the crack set. We consider asymmetry to be potentially very attractive in engineering critical components as methods of synthesis enable closer control of microstructure. The role of asymmetry in surface properties, and its exploitation in both nature and in engineering, is only now being recognized (e.g., Malvadkar et al., 2010; Xia et al., 2012, 2013). We believe that similar opportunities exist in fracture.

Effective toughness vs. effective surface area. Our examples demonstrate that *effective toughness is different from the weighted surface area*. In the examples of stripes (Section 5) and asymmetric microstructure (Section 8), the crack remains straight and thus the surface area remains unchanged; yet the toughness is different. In the example in Section 7, the crack may meander, yet the toughness is again different from the overall area. We provide an additional example in Section 6 with layers of alternating toughness but uniform elastic modulus subjected to Mode-I loading perpendicular to the layers. The crack propagates in a straight manner, but the effective toughness is equal to the higher of the two toughnesses as opposed to the average.

Enhanced dissipation. The fact that the *effective toughness is defined by the peak and not the average driving force* is an important assertion of our work. Physically, the peak driving force is what one would have to apply before the crack can propagate through macroscopic distances. A macroscopic device would not have the sensitivity to respond and relax at the microscopic time-scales for the system to be able to recover the energy when the crack propagates discontinuously. There would be dynamic effects and these would also lead to a loss.

In this context, we observe that the model we use has a variational structure and specifically has energy conservation for smooth propagation (Bourdin et al., 2000, 2008). However, in heterogeneous materials, the crack set does not necessarily grow smoothly and thus one does not necessarily have any energy conservation. Consequently, the macroscopic dissipation can be strictly larger than the microscopic dissipation.

Open issues and extensions: Underlying our formulation is a conjectured homogenization result that effective toughness is indeed well defined and that our surfing boundary condition does compute the effective toughness. In this work, we have provided computational support for this conjecture, but a rigorous proof remains open. A closely related issue is that we use the J-integral on the boundary to compute the effective toughness. Implicit in this idea is a conjecture that the J-integral converges to a definite value as we go far away from the crack set. This remains an open question. The J-integral can be path dependent in a heterogeneous material. Furthermore, the J-integral as well as the underlying Eshelby energy-momentum tensor is quadratic in quantities that are fluctuating. While cancelations (Hill's lemma or div-curl lemma) give rise to convergence in some quadratic terms including the energy density, this is not clear for the second term $(\nabla u)^T \sigma$. We note that mechanical equilibrium implies a controlled divergence of the Eshelby energy-momentum tensor, and this may indeed provide some cancelations, but we have been unable to prove this. In this work, we minimize this difficulty by including a padded region with effective modulus. Fig. 17 shows the J-integral computed on three paths, at the outer boundary of the padded regions, at the inner boundary of the padded region and though the interior of the heterogeneous material. The first two agree exactly as one would expect, but so does the third. Additionally, we have repeated many of our calculations with larger domains and verified that our results remain unchanged (e.g. Fig. 6(d)).

In many of our examples, crack re-nucleation plays a critical role. Thus, the overall toughness is dictated by the crack-initiation criterion. A systematic understanding of crack-initiation criterion and how this arises from the atomistic and microstructural scale remains a work in progress. In this work, we have used a regularized model of fracture, and this involves a regularization parameter ε that controls crack initiation (Bourdin et al., 2014).

The examples presented in this work are limited to macroscopic crack propagation in principal directions (symmetry planes) of the microstructure. In situations where the crack is driven in arbitrary directions, the anisotropy in toughness can lead to crack faceting on a scale larger than that of the microstructure, but smaller than the microscopic scale. Similarly, in the examples presented here, we have not considered situations where the interfacial toughness is different from the bulk values. In such situations, the crack can deviate into the interface, as shown for example in the work of He and Hutchinson for the example in Section 5.2. Furthermore, the examples presented here do not consider situations where the microcracks nucleate remotely from the main crack. Finally, we have not considered anisotropic fracture toughness. We are currently using the framework proposed here to study these situations, and the results will be presented elsewhere.

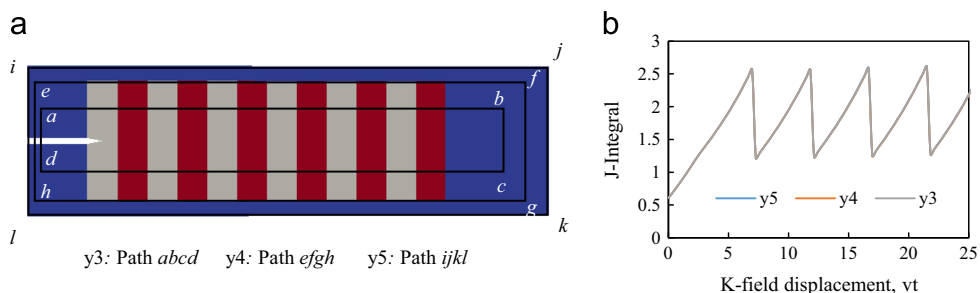


Fig. 17. J-integral computed on various contours.

Acknowledgments

We have greatly benefited from many discussions with Chris J. Larsen and G. “Ravi” Ravichandran, and are grateful for their insights, criticism and encouragement. We are also grateful for the insightful comments of the reviewers. MZH, C-JH and KB gratefully acknowledge the financial support of the U.S. National Science Foundation (Grant No. CMMI-1201102). BB's work was supported in part by the National Science Foundation Grant No. DMS-0909267. Some numerical experiments were performed using resources of the Extreme Science and Engineering Discovery Environment (XSEDE), which is supported by National Science Foundation grant number OCI-1053575 under the Resource Allocation TG- DMS060014, and some using the Garuda Computational Cluster which are partially funding through a DURIP grant from the US Army Research Office.

References

- Abeyaratne, R., Chu, C., James, R.D., 1996. Kinetics of materials with wiggly energies: theory and application to the evolution of twinning microstructures in a Cu–Al–Ni shape memory alloy. *Philos. Mag.* A 73, 457–497.
- Ambrosio, L., Tortorelli, V.M., 1990. Approximation of functional depending on jumps by elliptic functional via t -convergence. *Comm. Pure Appl. Math.* 43, 999–1036.
- Atkinson, C., 1975. On the stress intensity factors associated with cracks interacting with an interface between to elastic media. *Int. J. Eng. Sci.* 13, 489–504.
- Balay, S., Brown, J., Buschelman, K., Eijkhout, V., Gropp, W.D., Kaushik, D., Knepley, M.G., Curfman McInnes, L., Smith, B.F., Zhang, H. PETSc Users Manual. Technical Report ANL-95/11—Revision 3.4, Argonne National Laboratory, 2013.
- Balay, S., Brown, J., Buschelman, K., Gropp, W.D., Kaushik, D., Knepley, M., McInnes, L.C., Smith, B., Zhang, H., 2013. PETSc Web page. (<http://www.mcs.anl.gov/petsc>).
- Balay, S., Gropp, W., Curfman McInnes, L., Smith, B., 1997. Efficient management of parallelism in object oriented numerical software libraries. In: Arge, E., Bruaset, A.M., Langtangen, H.P. (Eds.), *Modern Software Tools in Scientific Computing*. Birkhäuser Press, Cambridge, MA, USA, pp. 163–202.
- Barthelat, F., Espinosa, H.D., 2007. An experimental investigation of deformation and fracture of nacre—mother of pearl. *Exp. Mech.* 47, 311–324.
- Begley, M.R., Phillips, N.R., Compton, B.G., Wilbrink, D.V., Ritchie, R.O., Utz, M., 2012. Micromechanical models to guide the development of synthetic ‘brick and mortar’ composites. *J. Mech. Phys. Solids* 60, 1545–1560.
- Bhattacharya, K., 1999. Phase boundary propagation in a heterogeneous body. *Philos. R. Soc. Lond. A* 455, 757–766.
- Bonamy, D., Ponson, L., Prades, S., Bouchaud, E., Guillot, C., 2006. Scaling exponents for fracture surfaces in homogeneous glass and glassy ceramics. *Phys. Rev. Lett.* 97, 135504.
- Bonamy, D., Santucci, S., Ponson, L., 2008. Crackling dynamics in material failure as the signature of a self-organized dynamic phase transition. *Phys. Rev. Lett.* 101, 045501.
- Bouchaud, E., 1997. Scaling properties of cracks. *J. Phys. Condens. Mat.* 9, 4319–4344.
- Bourdin, B., Francfort, G., Marigo, J.-J., 2000. Numerical experiments in revisited brittle fracture. *J. Mech. Phys. Solids* 48, 797–826.
- Bourdin, B., Francfort, G., Marigo, J.-J., 2008. The variational approach to fracture. *J. Elast.* 91, 1–148.
- Bourdin, B., Marigo, J.-J., Maurini, C., Sicsic, P., 2014. Morphogenesis and propagation of complex cracks induced by thermal shocks. *Phys. Rev. Lett.* 112, 014301.
- Bower, A., Ortiz, M., 1991. A 3-dimensional analysis of crack trapping and bridging by tough particles. *J. Mech. Phys. Solids* 39, 815–858.
- Bueckner, H.F., 1970. A novel principle for the computation of stress intensity factors. *Z. Angew. Math. Mech.* 50, 529–546.
- Cherepanov, G.P., 1967. Crack propagation in continuous media. *J. Appl. Math. Mech.* 31, 503–512.
- Cox, B., Yang, Q., 2006. In quest of virtual tests for structural composites. *Science* 314, 1102–1107.
- Currey, J.D., Taylor, J.D., 1974. Mechanical-behavior of some molluscan hard tissues. *J. Zool.* 173, 395–406.
- Dirr, N., Yip, N.K., 2006. Pinning and de-pinning phenomena in front propagation in heterogeneous media. *Interface Free Bound.* 8, 79–109.
- Dondle, P., Bhattacharya, K., 2014. Effective behavior of an interface propagating through a periodic elastic medium. In preparation.
- Evans, A.G., Faber, K.T., 1981. Toughening of ceramics by circumferential microcracking. *J. Am. Ceram. Soc.* 64, 394–398.
- Evans, A.G., Suo, Z., Wang, R.Z., Aksay, I.A., He, M.Y., Hutchinson, J.W., 2001. Model for the robust mechanical behavior of nacre. *J. Mater. Res.* 16, 2475–2484.
- Faber, K.T., Evans, A.G., 1983. Crack deflection processes. 1. Theory. *Acta Metall. Mater.* 31, 565–576.
- Faber, K.T., Evans, A.G., 1983. Crack deflection processes. 2. Experiment. *Acta Metall. Mater.* 31, 577–584.
- Francfort, G., Marigo, J.-J., 1998. Revisiting brittle fracture as an energy minimization problem. *J. Mech. Phys. Solids* 46, 1319–1342.
- Freund, L.B., 2014. Brittle crack growth modeled as the forced separation of chemical bonds within a K-field. *J. Mech. Phys. Solids* 64, 212–222.
- Gao, H., 1991. Fracture-analysis of nonhomogeneous materials via a moduli-perturbation approach. *Int. J. Solids Struct.* 27, 1663–1682.
- Gao, H., Rice, J., 1989. A first-order perturbation analysis of crack trapping by arrays of obstacles. *J. Appl. Mech.* 56, 828–836.
- Griffith, A.A., 1921. The phenomena of rupture and flow in solids. *Phil. Trans. R. Soc. Lond.* 221, 193–198.
- Gurtin, M.E., Podio-Guidugli, P., 1996. Configurational forces and the basic laws for crack propagation. *J. Mech. Phys. Solids* 44, 905–927.
- He, M.Y., Hutchinson, J.W., 1989. Crack deflection at an interface between dissimilar elastic materials. *Int. J. Solids Struct.* 25, 1053–1067.
- Holland, D., Marder, M., 1998. Ideal brittle fracture of silicon studied with molecular dynamics. *Phys. Rev. Lett.* 80, 746–749.
- Hutchinson, J., Suo, Z., 1992. Mixed-mode cracking in layered materials. *Adv. Appl. Mech.* 29 (Jan.), 63–191.
- Irwin, G.R., 1957. Analysis of stresses and strains near the end of a crack traversing a plate. *J. Appl. Mech.* 24, 361–364.
- Kermode, J.R., Albaret, T., Sherman, D., Bernstein, N., Gumbsch, P., Payne, M.C., Csanyi, G., Vita, A.D., 2008. Low-speed fracture instabilities in a brittle crystal. *Nature* 455, 1224–1227.
- Knowles, J.K., 1981. A note on the energy-release rate in quasi-static elastic crack-propagation. *SIAM J. Appl. Math.* 41, 401–412.
- Malvadkar, N.A., Hancock, M.J., Sekeroglu, K., Dressick, W.J., Demirel, M.C., 2010. An engineered anisotropic nanofilm with unidirectional wetting properties. *Nat. Mater.* 9, 1023–1028.
- Menig, R., Meyers, M.H., Meyers, M.A., Vecchio, K.S., 2000. Quasi-static and dynamic mechanical response of *Haliotis rufescens* (abalone) shells. *Acta Mater.* 48, 2383–2398.
- Milton, G., 2002. *The Theory of Composites*. Cambridge University Press, Cambridge, England.
- Munson, T., Sarich, J., Wild, S., Benson, S., McInnes, L.C., 2012. Tao 2.0 Users Manual. Technical Report ANL/MCS-TM-322, Mathematics and Computer Science Division, Argonne National Laboratory. (<http://www.mcs.anl.gov/tao>).
- Nemat-Nasser, S., Hori, M., 1999. *Micromechanics: Overall Properties of Heterogeneous Materials*. Elsevier Science, North-Holland, The Netherlands.
- Nukala, P.K.V.V., Simunovic, S., 2005. Statistical physics models for nacre fracture simulation. *Phys. Rev. E* 72, 041919.
- Ponson, L., Bonamy, D., 2010. Crack propagation in brittle heterogeneous solids: material disorder and crack dynamics. *Int. J. Fract.* 162, 21–31.
- Ramanathan, S., Ertas, D., Fisher, D.S., 1997. Quasistatic crack propagation in heterogeneous media. *Phys. Rev. Lett.* 79, 873–876.
- Rice, J., 1985. 1st-order variation in elastic fields due to variation in location of a planar crack front. *J. Appl. Mech.* 52, 571–579.

- Rice, J.R., 1968. A path independent integral and the approximate analysis of strain concentration by notches and cracks. *J. Appl. Mech.* 35, 379–386.
- Srivastava, A., Ponson, L., Osovski, S., Bouchaud, E., Needleman, A., 2014. Effect of inclusion density on ductile fracture toughness and roughness. *J. Mech. Phys. Solids* 63, 62–79.
- Suresh, S., 1985. Fatigue crack deflection and fracture surface-contact—micromechanical models. *Metall. Trans. A* 16, 249–260.
- Xia, S., Ponson, L., Ravichandran, G., Bhattacharya, K., 2012. Toughening and asymmetry in peeling of heterogeneous adhesives. *Phys. Rev. Lett.* 108, 196101.
- Xia, S.M., Ponson, L., Ravichandran, G., Bhattacharya, K., 2013. Adhesion of heterogeneous thin films—I elastic heterogeneity. *J. Mech. Phys. Solids* 61, 838–851.
- Zak, A.R., Williams, M.L., 1963. Crack point stress singularities at a bi-material interface. *J. Appl. Mech.* 30, 142–143.
- Zehnder, A.T., 2012. Fracture Mechanics. In: *Lecture Notes in Applied and Computational Mechanics*, No 62. Springer-Verlag.